Journal of Structural Geology 31 (2009) 759–775

Contents lists available at ScienceDirect

Journal of Structural Geology

journal homepage: www.elsevier.com/locate/jsg

Geometry and architecture of faults in a syn-rift normal fault array: The Nukhul half-graben, Suez rift, Egypt

Paul Wilson [a,*], Rob L. Gawthorpe [a], David Hodgetts [a], Franklin Rarity [a], Ian R Sharp [b]

[a] Basin Studies and Petroleum Geoscience, School of Earth, Atmospheric and Environmental Sciences, University of Manchester, Williamson Building, Oxford Road, Manchester M13 9PL, United Kingdom
[b] StatoilHydro Research Center, Sandsliveien 90, Bergen, N-5020, Norway

ARTICLE INFO

Article history:
Received 22 February 2008
Received in revised form
9 April 2009
Accepted 14 April 2009
Available online 23 April 2009

Keywords:
Normal faults
Fault propagation
Fault architecture
Fault geometry
Rifts
Suez rift

ABSTRACT

The geometry and architecture of a well exposed syn-rift normal fault array in the Suez rift is examined. At pre-rift level, the Nukhul fault consists of a single zone of intense deformation up to 10 m wide, with a significant monocline in the hanging wall and much more limited folding in the footwall. At syn-rift level, the fault zone is characterised by a single discrete fault zone less than 2 m wide, with damage zone faults up to approximately 200 m into the hanging wall, and with no significant monocline developed. The evolution of the fault from a buried structure with associated fault-propagation folding, to a surface-breaking structure with associated surface faulting, has led to enhanced bedding-parallel slip at lower levels that is absent at higher levels. Strain is enhanced at breached relay ramps and bends inherited from pre-existing structures that were reactivated during rifting. Damage zone faults observed within the pre-rift show ramp-flat geometries associated with contrast in competency of the layers cut and commonly contain zones of scaly shale or clay smear. Damage zone faults within the syn-rift are commonly very straight, and may be discrete fault planes with no visible fault rock at the scale of observation, or contain relatively thin and simple zones of scaly shale or gouge. The geometric and architectural evolution of the fault array is interpreted to be the result of (i) the evolution from distributed trishear deformation during upward propagation of buried fault tips to surface faulting after faults breach the surface; (ii) differences in deformation response between lithified pre-rift units that display high competence contrasts during deformation, and unlithified syn-rift units that display low competence contrasts during deformation, and; (iii) the history of segmentation, growth and linkage of the faults that make up the fault array. This has important implications for fluid flow in fault zones.

1. Introduction

Fault zone architecture, defined as the three-dimensional spatial arrangement of structural elements such as zones of fault rock (e.g. gouge or cataclasite), lenses of wall rock incorporated into the fault zone, and damage zones fringing the fault zone (Hancock, 1985; Wilson, 2008), is both temporally and spatially variable. Such variability results from fault zones cutting different rock types (e.g. Yielding et al., 1997), bifurcation of faults during their evolution (e.g. Childs et al., 1996a), the growth and linkage of fault segments through time (e.g. Cartwright et al., 1995; Cowie et al., 2000; Gawthorpe et al., 2003), and the variation in local stress environment along the fault (e.g. at restraining or releasing bends; Sibson, 1986).

In rift basins, it would be expected that the architectural characteristics of faults will change significantly as faults initiate in basement or in lithified pre-rift units, propagate vertically into unlithified syn-rift units, break the surface, and propagate laterally to link with adjacent fault segments (e.g. Heynekamp et al., 1999; Sigda et al., 1999; Gawthorpe and Leeder, 2000; Sharp et al., 2000a, b; Rawling et al., 2001; Gawthorpe et al., 2003). Several publications have addressed the influence of lithology ('mechanical stratigraphy': Erickson, 1996) on the geometry and architecture of faults and fault-related folds (e.g. Withjack et al., 1990; Dominic and McConnell, 1994; Pascoe et al., 1999; Cardozo et al., 2005; Jackson et al., 2006; Schöpfer et al., 2006, 2007), but the influence of the degree of lithification of the protolith on fault geometry and architecture is not well understood. The temporal evolution of the faults, coupled with the changing nature of the rocks being faulted (i.e. lithified pre-rift units followed by poorly lithified syn-rift units) should lead to significant spatial variation in fault architecture in the final fault array. However, it is rarely possible to make

* Corresponding author: Fax: +44 0 161 306 9361.
E-mail address: paul.wilson@manchester.ac.uk (P. Wilson).

0191-8141/$ – see front matter © 2009 Elsevier Ltd. All rights reserved.
doi:10.1016/j.jsg.2009.04.005

observations of fault geometry and architecture over half-graben scale (several km^2) syn-depositional fault arrays in the field. Indeed, despite great interest in the issue of how faults affect fluid flow in the crust, relatively few field descriptions of faults are available in the public domain. In this study we present observations of an exceptionally well exposed fault array and associated syn-rift and pre-rift strata in the Nukhul half-graben of the Suez rift, Egypt (Fig. 1). There are two sets of observations. The first set comprises observations of the geometry and architecture of an intra-block normal fault (the Nukhul fault) at different localities along strike. The second comprises observations of a set of minor normal faults within the footwall damage zone of a major block-bounding fault (the Baba-Markha fault) at both pre-rift and syn-rift level. Our field observations are placed in the context of a half-graben scale terrestrial LIDAR dataset (see Section 3), in which key stratigraphic horizons and faults can be mapped very accurately. This allows a reconstruction of the evolution of the half-graben and in particular the vertical and lateral propagation of faults (Wilson et al., 2009). Our purpose in this paper is as follows:

(i) to describe the geometry and architecture of the fault array in the Nukhul half-graben;
(ii) to discuss how the temporal evolution of the fault array, in terms of vertical and lateral propagation and linkage of faults, has affected the geometry and architecture of the fault array, and;
(iii) to discuss how lithology (including state of lithification) has controlled the geometry and architecture of the fault array.

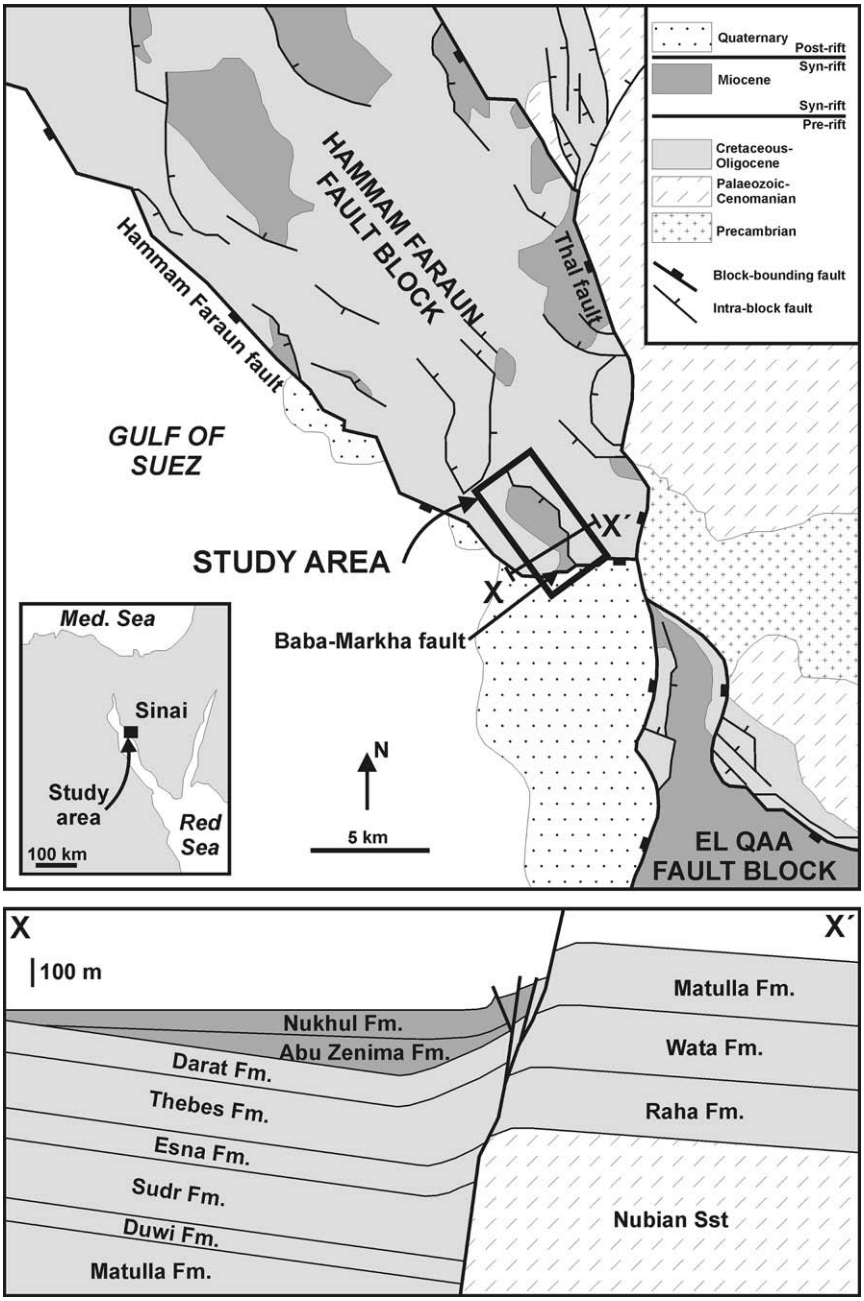

Fig. 1. Simplified geological map of the Hammam Faraun and El Qaa fault blocks, Suez rift, showing the location of the study area. The cross section shows the geometry of pre-rift and syn-rift units in the half-graben bounded by the Nukhul fault. Modified after Moustafa and Abdeen (1992), Jackson et al. (2006) and I.R. Sharp (unpublished).

2. Geological setting and stratigraphy

The Suez Rift is the northwest extension of the Red Sea rift. It developed in Oligo-Miocene time as a result of the separation of the Arabian and African plates (e.g. Garfunkel and Bartov, 1977; Lyberis, 1988; Patton et al., 1994). The rift is approximately 300 km long and up to 80 km wide and is characterised by normal faults defining tilted fault blocks. The rift has been divided into three dip provinces characterised by their differing fault polarity. In the northern and southern dip provinces normal faults dip dominantly to the northeast and strata dip dominantly to the southwest; in the central dip province normal faults dip dominantly to the southwest and strata dip dominantly to the northeast (Moustafa, 1993). The dip provinces are separated from each other by rift-transverse accommodation zones (Patton et al., 1994; Moustafa, 1996, 1997; Bosworth et al., 2005).

The Hammam Faraun fault block (Fig. 1) forms part of the central dip province. It is bounded to the east by the Thal fault and to the west by the Hammam Faraun fault (Fig. 1). These major block-bounding normal faults are in excess of 25 km long and dip steeply (60–80°) to the west (e.g. Moustafa, 1993). To the south, the block is bounded by the approximately east-striking Baba-Markha normal fault (Fig. 1). Estimated maximum throw magnitudes are 4800 m for the Hammam Faraun fault, 1850 m for the Thal fault and 3500 m for the Baba-Markha fault (Moustafa, 1993), although the Baba-Markha fault may have a minor component of sinistral strike-slip movement (Moustafa and Abdeen, 1992; Jackson et al., 2006). The Nukhul fault is an intra-block fault within the Hammam Faraun fault block. It bounds a half-graben containing Oligo-Miocene syn-rift sediments of the Abu Zenima and Nukhul formations (see below; Figs. 1 and 2).

The stratigraphy of the Hammam Faraun fault block is summarised in Fig. 3. Pre-rift strata in the study area comprise two megasequences (Robson, 1971; Moustafa, 1987; Sharp et al., 2000a; Jackson et al., 2006). Megasequence 1 consists of Nubian sandstones (Cambrian to Lower Cretaceous in age) that unconformably overlie Precambrian 'pan-African' basement. Megasequence 2 consists of a Cretaceous mixed carbonate-clastic succession (Raha, Wata, Matulla, Duwi and Sudr formations) overlain by a mixed carbonate–mudstone sequence of Palaeocene to Eocene age (Esna, Thebes, Darat, Thal, Tanka and Khaboba formations). The mechanical anisotropy resulting from the presence of intervals containing significant amounts of mudstone (particularly the Duwi, Esna and Darat formations) within the overall carbonate-dominated pre-rift succession is of critical importance to the structural evolution of the study area (Sharp et al., 2000a; Khalil and McClay, 2002; Jackson et al., 2006).

The pre-rift units are unconformably overlain by a clastic syn-rift succession (Megasequence 3) of Oligo-Miocene age (Garfunkel and Bartov, 1977; Patton et al., 1994). In the Nukhul half-graben the pre-rift/syn-rift unconformity is overlain by a basal syn-rift boulder conglomerate unit (Sharp et al., 2000a, b). The conglomerate contains clasts of pre-rift lithologies, showing that the pre-rift units were lithified at the onset of syn-rift deposition. At the present day, syn-rift units vary from poorly lithified (the Abu Zenima Formation) to relatively well indurated (the Nukhul Formation). The syn-rift units form an overall transgressive succession comprising the non-marine Abu Zenima Formation (24–21.5 Ma), the tidally influenced to marginal marine Nukhul Formation (21.5–19.7 Ma), and the open marine Rudeis Formation (19.7–15.5 Ma: ages based on Patton et al., 1994; Krebs et al., 1997). The Abu Zenima and Nukhul formations are separated by a local unconformity-correlative conformity (T05 surface of Krebs et al., 1997; Fig. 3).

3. Methodology

In this study a fault zone is defined by paired slip surfaces, such that any material between the bounding surfaces is classified as being part of the 'fault zone', regardless of the degree of deformation (Childs et al., 1996a, b). A 'damage zone' is here defined as a zone of deformed rock surrounding the fault zone in which deformation features have higher density than the 'background' away from the fault zone (e.g. McGrath and Davison, 1995; Kim et al., 2004).

This study utilises an integrated dataset comprising terrestrial LIDAR scan data (Bellian et al., 2005; Pringle et al., 2006; Redfern et al., 2007), linked to digital photography, satellite imagery and field observations (Wilson et al., 2009). This dataset allows key geological horizons to be mapped around the study area to a very high degree of accuracy (on the order of centimetres to tens of centimetres). Geological data derived from the LIDAR data can also easily be used in industry standard geological modelling software (in this case, Schlumberger's Petrel suite). These data enable us to create very accurate, high resolution structure contour and isopach maps of the stratigraphy in the study area. Faults were mapped onto 60-cm resolution Quickbird satellite images (Fig. 2). A fault model was built in Petrel using these data, and formed the structural basis for modelling key stratigraphic surfaces from the LIDAR data. This structural model enables reconstruction of the development of the fault array (Wilson et al., 2009). Where faults were well exposed, the orientation, displacement, geometry, juxtaposed rock types, and fault architecture were recorded. Fault architecture was described in terms of presence or absence of fault rock, and the thickness, lithology and continuity of the fault rock if present; and the presence or absence of a damage zone, the thickness of the damage zone, and intensity and orientation of faults and/or fractures within the damage zone.

4. The Nukhul half-graben

The Nukhul fault forms the eastern boundary of a half-graben filled with early syn-rift sediments of the Abu Zenima and Nukhul formations (Fig. 2). The half-graben defined by the Nukhul fault is bounded to the south by the Baba-Markha fault, that forms the southern margin of the Hammam Faraun fault block (Figs. 1 and 2). Fig. 4 shows cross-sections summarising the structural and stratigraphic relationships in the area of the Nukhul half-graben. The Nukhul fault dips moderately to steeply (50–75°) to the west or southwest and in plan view can be divided into five segments, based on the presence of sharp kinks in the fault trace along strike (Fig. 2). Projections of the top of the Darat Formation onto the fault plane indicate a maximum throw of approximately 1 km at the intersection with the Baba-Markha fault in the south, with throw overall decreasing northwards, over approximately 10 km, to a well-defined tip zone comprising a fault-tip monocline and fault splays (Sharp et al., 2000a; Gawthorpe et al., 2003; Wilson et al., 2009). Throw for the different fault segments is approximately 850–1000 m along segment 1, 700–850 m along segment 2, 600–650 m along segment 3, 500–600 m along segment 4 and zero (at the tip) to 500 m along segment 5 (Wilson et al., 2009).

Along segments 1 and 2, the fault juxtaposes the pre-rift Matulla and Wata formations in the footwall against the pre-rift Darat Formation in the hanging wall (Fig. 2; Fig. 4a). Along segments 3–5, the fault juxtaposes chalk of the pre-rift Sudr Formation in the footwall against syn-rift units in the hanging wall (Fig. 2; Fig. 4b, c). Hence from south to north, the exposed structural level of the fault zone becomes shallower. At the branch lines between segments 4 and 5, and segments 3 and 4, fault-perpendicular folds are observed in the hanging wall of the Nukhul fault (Fig. 5a, b). The fault-perpendicular folds are related to along-strike displacement variations along the Nukhul fault, and are interpreted to be related to the growth and linkage of initially isolated precursor fault segments that probably became linked within the first 2.5 m.y. of

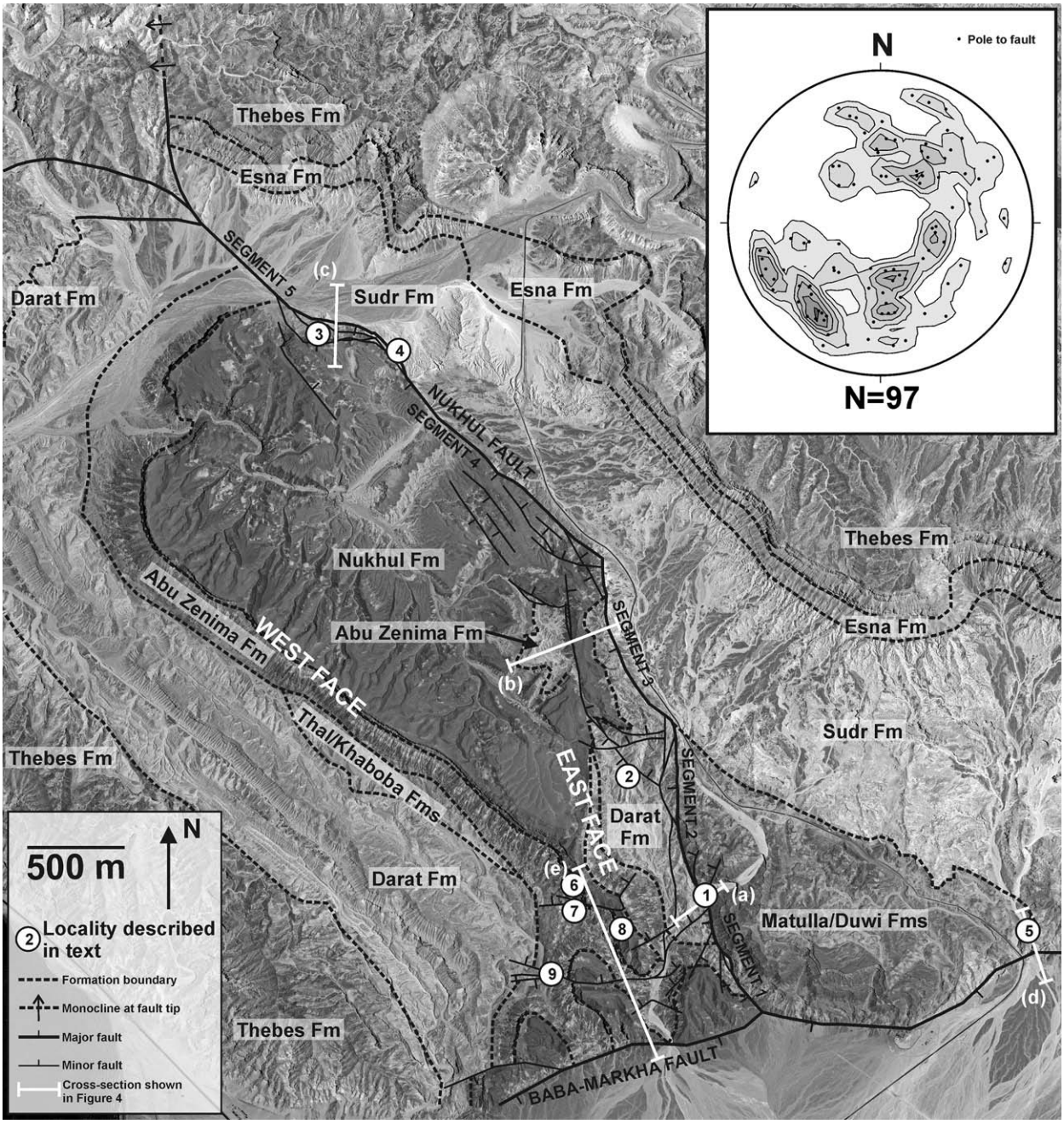

Fig. 2. Geological map of the Nukhul half-graben, showing faults, distribution of rock units, and localities described in the text. The stereonet shows poles to fault planes from the study area.

rifting (Wilson et al., 2009). A fault-parallel syncline occurs in the hanging wall of the Nukhul fault, while a fault-parallel anticline occurs in the footwall of the Baba-Markha fault; these folds interfere in the south, creating a saddle structure (Fig. 5a, b). The fault-parallel syncline associated with the Nukhul fault can be traced out into fault-tip monocline to the northwest (Fig. 2), suggesting that it is a fault-propagation fold, although it was likely modified by drag processes (Janecke et al., 1998; Sharp et al., 2000a).

Comparing the structure contour maps of the pre-rift/syn-rift contact (base Abu Zenima Formation: Fig. 5a) with the structure contour map for a key stratigraphic horizon within the Nukhul Formation (Fig. 5b), the fault-parallel monocline associated with the Nukhul fault is less pronounced in the Nukhul Formation. This change in structural style occurs abruptly at the surface separating the Abu Zenima and Nukhul formations, which is locally an angular unconformity (Fig. 3). This relationship can clearly be seen in Fig. 6a, where pre-rift and Abu Zenima Formation strata have much steeper dips than the relatively flat-lying Nukhul Formation. Isopach maps for representative intervals within the syn-rift strata show that the Abu Zenima Formation thins dramatically toward the Nukhul fault, while the Nukhul Formation does not display similar thinning (Fig. 5c, d). These data support the interpretation of Sharp et al. (2000a) that the Abu Zenima Formation was deposited in a monoclinal flexure ahead of the still-buried tip of the Nukhul fault prior to 21.5 Ma, while the Nukhul Formation was deposited after 21.5 Ma following the breaching of the surface by the Nukhul fault. This timing is not unequivocal, as there is presumably not an abrupt change in topography between the fault tip being close to the

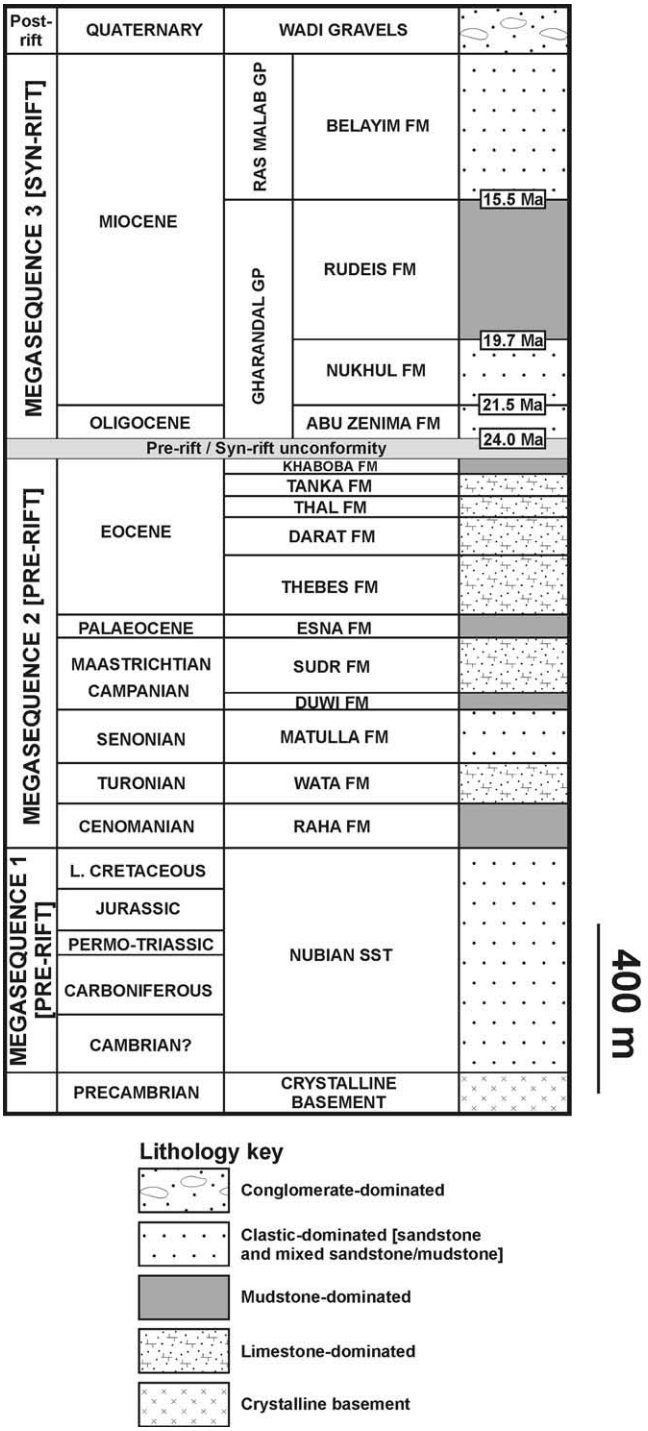

Fig. 3. Stratigraphic table for the Hammam Faraun and El Qaa fault blocks. Modified after Jackson et al. (2006).

surface and it actually breaching the surface, but it is at least broadly correct. Although the Nukhul Formation forms a fault-parallel syncline, it is clear from the abrupt change in dip at the contact between the Abu Zenima and Nukhul formations (Fig. 6a) that most of the folding in the hanging wall of the Nukhul fault occurred prior to Nukhul deposition.

Minor faults with throw magnitudes on the order of 10–100 m are well exposed in the Nukhul half-graben, and comprise three orientation sets (stereonet on Fig. 2). Approximately northwest-striking faults and approximately north-striking faults include the segments that make up the Nukhul fault. A set of approximately east-striking faults (including the Baba-Markha fault) is mainly restricted to the southernmost part of the field area, with minor faults forming a footwall damage zone to the Baba-Markha fault (Fig. 2; Fig. 4d, e). Normal faults, antithetic to the main Nukhul fault and typically 1–2 km in length, are developed in the Nukhul fault hanging wall (Fig. 2; Fig. 4b). These antithetic faults parallel the main Nukhul fault and are composed of NW–SE and N–S striking segments (Fig. 2a).

Previous work has shown that two phases of rifting, which can be tied to the activity of the evolving fault array, can be identified in the Hammam Faraun fault block. An early rift-initiation phase where a large number of relatively low-displacement faults were active, was followed by a rift climax phase where subsidence became localised onto the faults that became the present-day block-bounding structures (Garfunkel and Bartov, 1977; Richardson and Arthur, 1988; Patton et al., 1994; Krebs et al., 1997; Gawthorpe et al., 2003). As an intra-block fault, the Nukhul fault was one of the rift-initiation structures that became inactive by the onset of rift climax phase and deposition of the Rudeis Formation at around 19.7 Ma (Gawthorpe et al., 2003); no Rudeis Formation stratigraphy is preserved in the hanging wall of the fault. As a present-day block-bounding fault, the Baba-Markha fault continued to be active into the rift climax phase (Gawthorpe et al., 2003). Field mapping has shown that the contact between pre-rift and syn-rift units is erosive, and occurs at the level of the Darat, Thal, Tanka or Khaboba formations in the hanging wall of the Nukhul fault (Fig. 2). The oldest stratigraphic unit observed in the study area (the Wata Formation) was therefore buried by a maximum of 600 m of pre-rift strata at the onset of rifting, and no more than 800–900 m of pre-rift and syn-rift strata at any point during the evolution of the Nukhul half-graben. Thus for the exposures observed in this study, maximum depth of faulting is no more than 900 m. Some minor faults show thickening of syn-rift strata into their hanging walls and thinning onto their footwalls, suggesting that the minimum depth of faulting observed is on the order of a few metres.

5. Geometry and architecture of syn-rift faults

5.1. The Nukhul fault

5.1.1. Pre-rift level: segments 1 and 2

Along segments 1 and 2 (in the south of the study area), the Nukhul fault juxtaposes the pre-rift Matulla and Wata formations in the footwall against the pre-rift Darat Formation in the hanging wall. Thus, strata of the Wata, Matulla, Duwi, Sudr, Esna, Thebes and Darat formations have moved past each other across the fault along these fault segments (Fig. 3). The Matulla Formation consists of interbedded calcareous sandstone and shale, whereas the Darat Formation consists of chalky limestone beds 1–2 m thick, with shale interbeds 10 cm–5 m thick. Pre-rift strata in the hanging wall define the steep limb of a southwest-facing monocline, with dips increasing from 35° approximately 200 m southwest of the fault to 75–80° in the immediate hanging wall (Figs. 4a and 6a). In the footwall, steep dips are restricted to within 5 m of the fault trace (Fig. 6b), and minor synthetic normal faults are restricted to the area around the bend where segments 4 and 5 link (locality 1 on Fig. 2).

The architecture of the Nukhul fault zone at locality 1 (Fig. 2) is summarised in Fig. 6b. Paired slip surfaces delineate a fault zone approximately 10 m wide. A sharp footwall contact dipping 75° separates shallowly dipping Wata Formation protolith (nodular bedded limestone and dolomite) from the fault zone. The fault rock consists of dismembered beds up to 2 m long and 0.5 m wide bounded by steep faults of both reverse and normal displacement (Fig. 6b), surrounded by a matrix of deformed grey or brown mudstone with shaly foliation subparallel to the walls of the fault

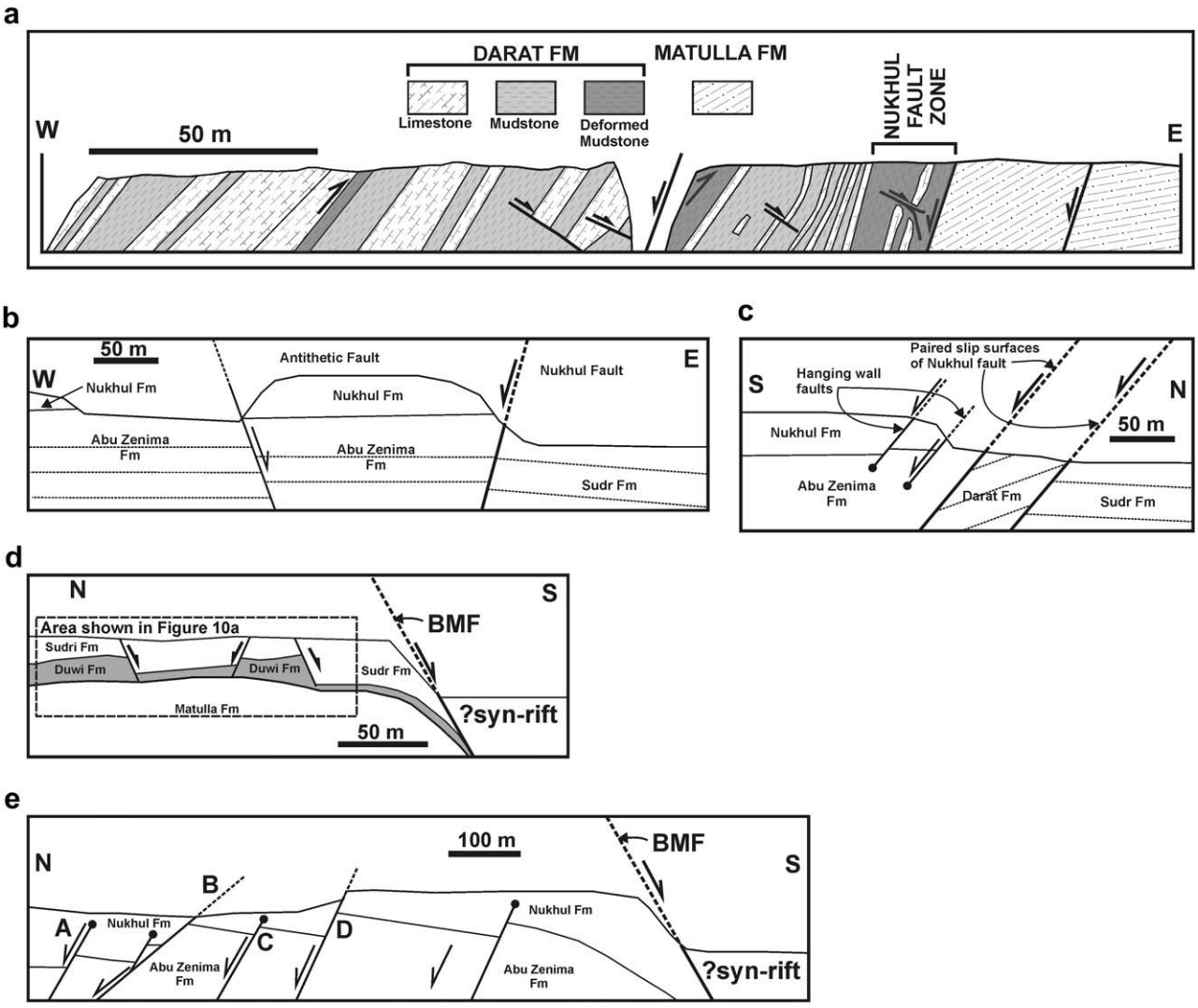

Fig. 4. Cross-sections illustrating the generalised structural geology and stratigraphy at the locations described in the text. The locations of the cross-sections are shown in Fig. 2.

zone. Minor folding (wavelength and amplitude on the centimetre scale) of the foliation is locally present. The shale is cut by a series of anastomosing fault-subparallel gouge zones, darker in colour than the surrounding shale, and between 5 and 10 mm thick. The gouge consists of clay with a distinct finely spaced (<1 mm) fracture cleavage that causes the rock to break into thin flakes. Fibrous gypsum veins up to 20 mm thick are subparallel to the foliation in the shale. They show little evidence of deformation, suggesting that they are relatively late features. Based on a sharp colour change in the shale and the type of dismembered blocks present, the fault zone can be divided into two parts. On the footwall side, dismembered beds are orange-red calcarenite of the Matulla Formation, while dark grey to maroon shale is probably derived from the Matulla and/or Duwi formations. On the hanging wall side, dismembered beds consist of buff limestone derived from the Darat Formation, and the shale matrix is light grey to brown in colour, similar to the Darat Formation in the immediate hanging wall.

In the hanging wall of the fault zone, an approximately 100 m wide damage zone within the Darat Formation is exposed. The damage zone consists of bedding-parallel deformation zones localised in shale beds, low-angle antithetic normal faults, and high-angle antithetic normal and reverse faults (Figs. 4a and 6a). Bedding-parallel deformation zones are defined by deformed shale with foliation subparallel to bedding and containing minor folds, anastomosing clay gouge zones and late, foliation-parallel, fibrous gypsum veins. It is suggested that these bedding-parallel deformation zones are related to flexural slip folding associated with monocline development in the hanging wall of the Nukhul fault. A series of low-angle normal faults with dip generally in the range 30–40° are observed within the damage zone (for example, at locality 2: see Figs. 2 and 7). These normal faults have unusual orientations when compared with most normal faults, which tend to have dip of approximately 60°, and are only found in areas where bedding is relatively steep due to monocline development. When the low-angle faults are rotated to bring bedding back to the horizontal, they are seen to be dominantly moderately to steeply northeast-dipping, northwest-striking structures (Figs. 7 and 8). This is consistent with the faults having initiated as antithetic structures in the hanging wall of the Nukhul fault, at a relatively early stage of faulting when bedding was relatively flat-lying. The faults were then rotated into low-angle orientations during monocline formation (Sharp et al., 2000a; Wibberley et al., 2007).

From locality 1, segment 2 of the Nukhul fault can be traced approximately 800 m to the north and segment 1 can be traced approximately 400 m to the south. The fault zone itself is incompletely exposed away from locality 1, but it is less clearly defined

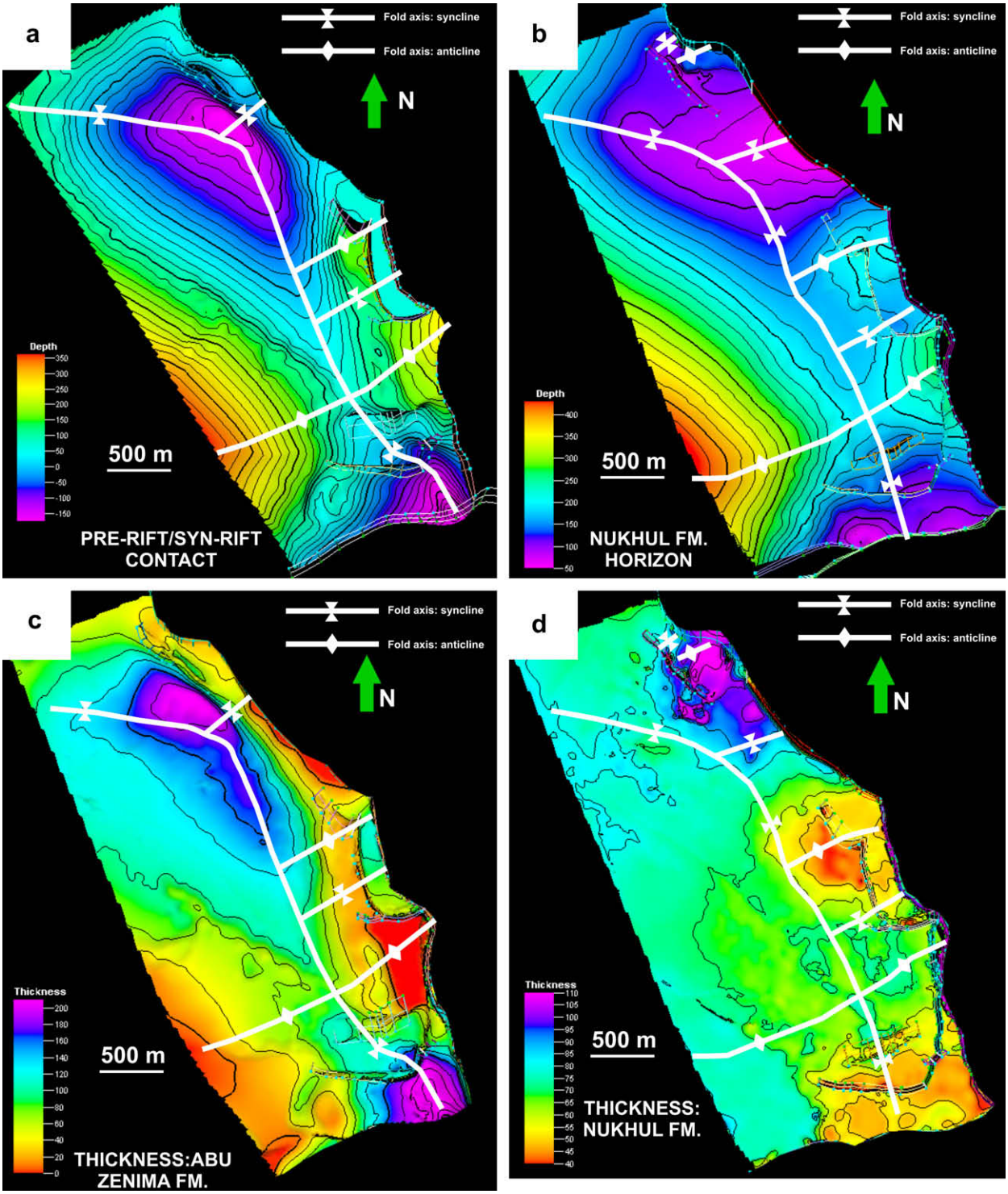

Fig. 5. LIDAR derived structure contour maps and isopach maps of key surfaces and intervals in the Nukhul half-graben. (a) Structure contour map of the pre-rift/syn-rift contact, showing the positions of fault-related folds. (b) Structure contour map of a key horizon within the Nukhul Formation, showing the positions of fault-related folds. The monocline that parallels the Nukhul fault is less pronounced than in (a). (c) Isopach map for the Abu Zenima Formation, showing dramatic thinning of the unit towards the Nukhul fault. Deposition of the Abu Zenima Formation was controlled by a monocline overlying the buried tip of the Nukhul fault. (d) Isopach map for a key interval within the lower part of the Nukhul Formation, showing no thinning toward the Nukhul fault. This suggests that the Nukhul fault had broken the surface during the deposition of the Nukhul Formation.

and narrower, up to 2 m wide, than at locality 1. However, the architectural style of the fault, characterised by dismembered wall rock derived blocks surrounded by a scaly shale matrix cut by anastomosing gouge zones, is consistent everywhere it can be observed along segments 1 and 2.

5.1.2. The Nukhul fault at syn-rift level: segments 3, 4 and 5

Along segments 3, 4 and 5 of the Nukhul fault (Fig. 2), chalk of the pre-rift Sudr Formation in the footwall is juxtaposed against the syn-rift Abu Zenima and Nukhul formations in the hanging wall. Strata of the Sudr, Esna, Thebes and Darat formations have

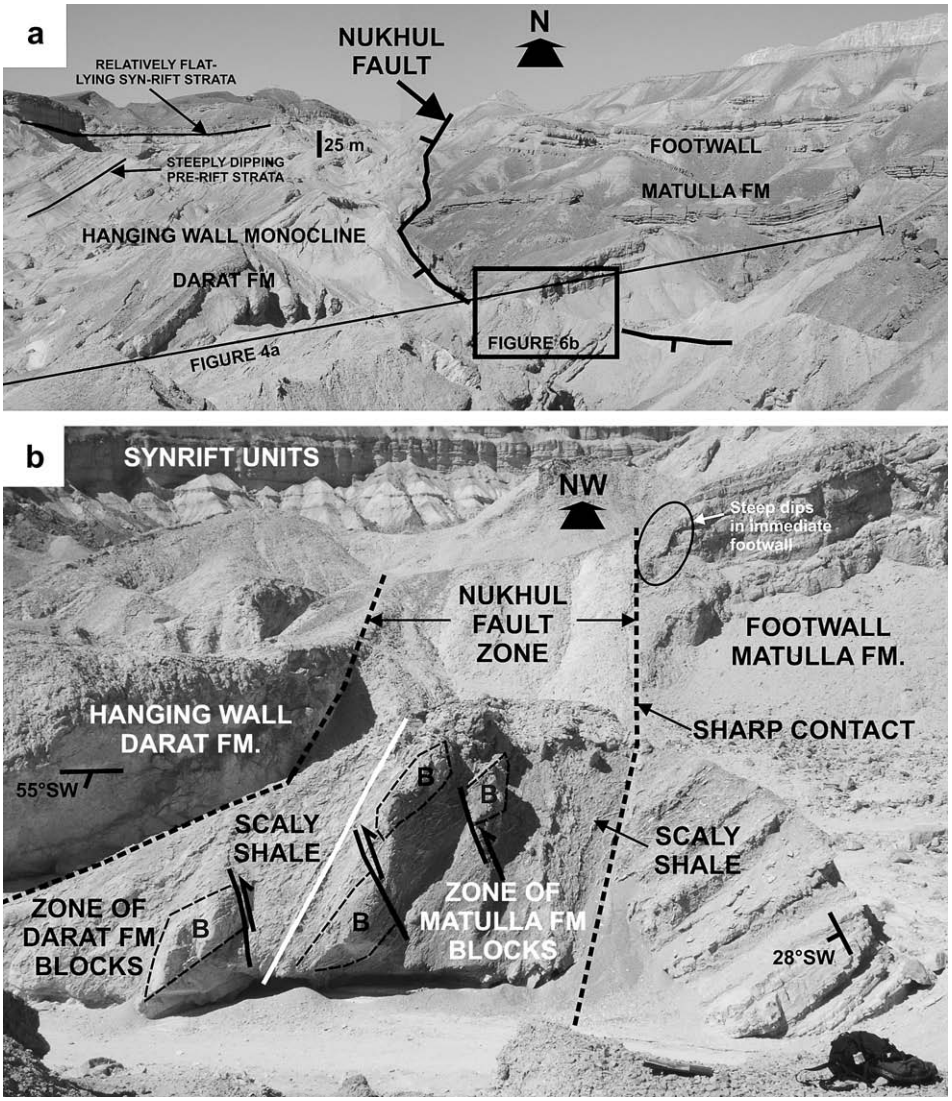

Fig. 6. Geometry and architecture of the Nukhul fault where it juxtaposes pre-rift strata against pre-rift strata (locality 1, Fig. 2). (a) Photopanorama showing the macro-scale geometry of the Nukhul fault. (b) Architecture of the Nukhul fault at locality 1. B, dismembered limestone blocks within the fault damage zone.

therefore moved past one another along these segments of the fault (Fig. 3).

Although the Nukhul fault zone is not well exposed along segments 3 and 4, field mapping shows that there is a series of synthetic and antithetic faults in the hanging wall of the fault within 200 m of the fault trace (Fig. 2). No faults are mapped in the footwall of the Nukhul fault along these segments (Fig. 2). The fault zone itself is narrow (<2 m wide), and has strong bends at the linkage points between segments 2 and 3, and segments 3 and 4 of the fault. Segments 1 and 2 of the fault are connected by a short (~600 m), approximately east-striking fault, along which good exposures are available (localities 3 and 4; Figs. 2, 4c and 9). The linking fault dips approximately 50° to the south. In the footwall, the Sudr Formation is not folded, with tilting of the footwall block imparting a shallow dip of bedding to the northeast, away from the Nukhul fault (Fig. 9). Paired slip surfaces bound a block of Darat Formation. The main slip surface, in the footwall of the Darat Formation block, separates pre-rift Sudr Formation from pre-rift Darat Formation, and therefore has a displacement of between 200 and 450 m. The second slip surface in the hanging wall of the fault zone separates the Darat Formation from syn-rift strata, and has a displacement of less than 100 m. Total displacement across the fault zone here is approximately 500 m (Gawthorpe et al., 2003; Wilson et al., 2009). Bedding within the sliver of Darat Formation in the fault zone strikes parallel to the fault, but the magnitude of dip is lower than that of the fault (30–40°; Fig. 9). The Darat Formation sliver can be traced for 600 m along strike, along the entire length of the fault that links segments 4 and 5, but is not observed along segment 4 (and segment 5 is buried underneath Wadi Nukhul). The Darat block in the fault zone is internally deformed, with faults synthetic to the bounding faults cutting steeply through limestone benches of the Darat Formation and soling into mudstone layers (Fig. 9b). At locality 3 (Fig. 2), the Nukhul Formation is folded into a monocline immediately adjacent to the fault with dip of up to 35° (Fig. 9b), but this relatively steep dip dies out within 10–20 m of the fault trace, in contrast to monoclinal folds at the pre-rift level where steep dips occur hundreds of metres away from the fault trace (Fig. 6a).

In the hanging wall of the second splay and within approximately 50 m of the fault trace, the Nukhul fault damage zone, consisting of synthetic faults with normal displacements of <5 m, is exposed. The faults are discrete with no fault rock visible. The faults lose displacement and tip out downward (Fig. 9a). In the footwall of the

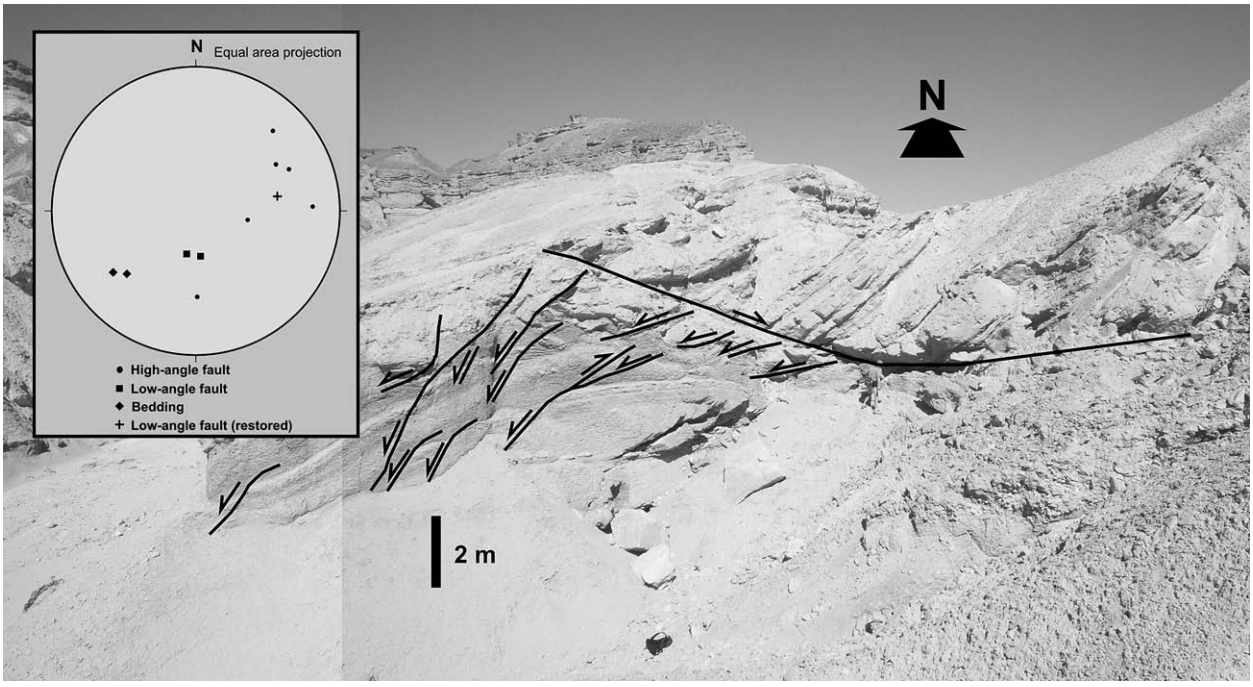

Fig. 7. A low-angle fault exposed in the steep limb of the monocline in the hanging wall of the Nukhul fault (locality 2, Fig. 2).

Nukhul fault zone, the damage zone consists of two parts. Directly adjacent to the fault, there is 2–5 m of intensely fractured Sudr Formation chalk (Fig. 9c). Fractures are anastomosing and fracture spacing is on the order of 1–2 cm, leading to the rock breaking up into internally undeformed lensoid fragments. Adjacent to this intensely fractured zone is a region of faulted chalk up to 10 m wide. Faults in this zone have spacing on the order of a few centimetres to several tens of centimetres, and displacements on the order of a few cm.

5.2. The footwall damage zone of the Baba-Markha fault

Two cross-sections illustrating the damage zone in the footwall of the Baba-Markha fault (displacement approximately 3500 m; Moustafa, 1993) in two different areas are shown in Fig. 4d and e. Fig. 4d illustrates the damage zone as exposed in pre-rift units, while Fig. 4e illustrates the damage zone in as exposed in syn-rift units.

5.2.1. The damage zone in pre-rift strata

Deformation of pre-rift units in the footwall damage zone of the block-bounding Baba-Markha fault, approximately 100 m north of the fault trace, is observed at locality 5 (Fig. 2; Fig. 4d; Fig. 10). At this locality, interbedded calcareous sandstone and shale of the Matulla Formation is overlain by the mudstone-dominated Duwi Formation and chalk of the Sudr Formation (Fig. 10a). The faults at this locality have a distinct ramp-flat geometry. Displacement varies from a few centimetres to approximately 10 m. Discrete fault planes cut steeply

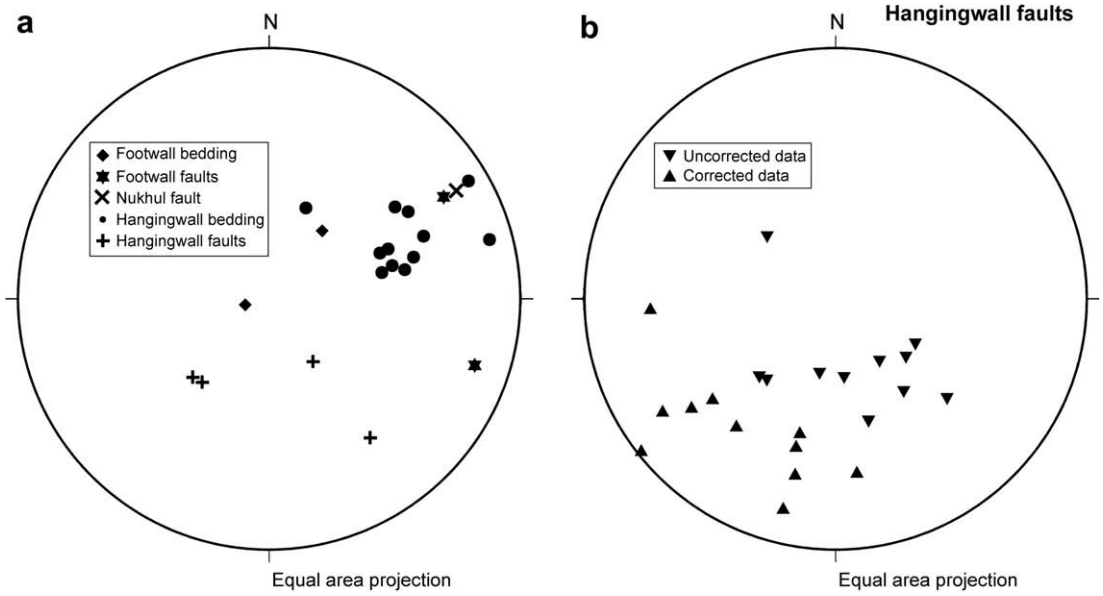

Fig. 8. Stereonets illustrating the orientations of structural features along segments 1 and 2 of the Nukhul fault (Fig. 2). (a) Orientation of structural elements along segment 4. (b) Orientation of low-angle faults in the hanging wall of the Nukhul fault, and orientation of the faults when the bedding they displace (Darat Formation) is restored to the horizontal.

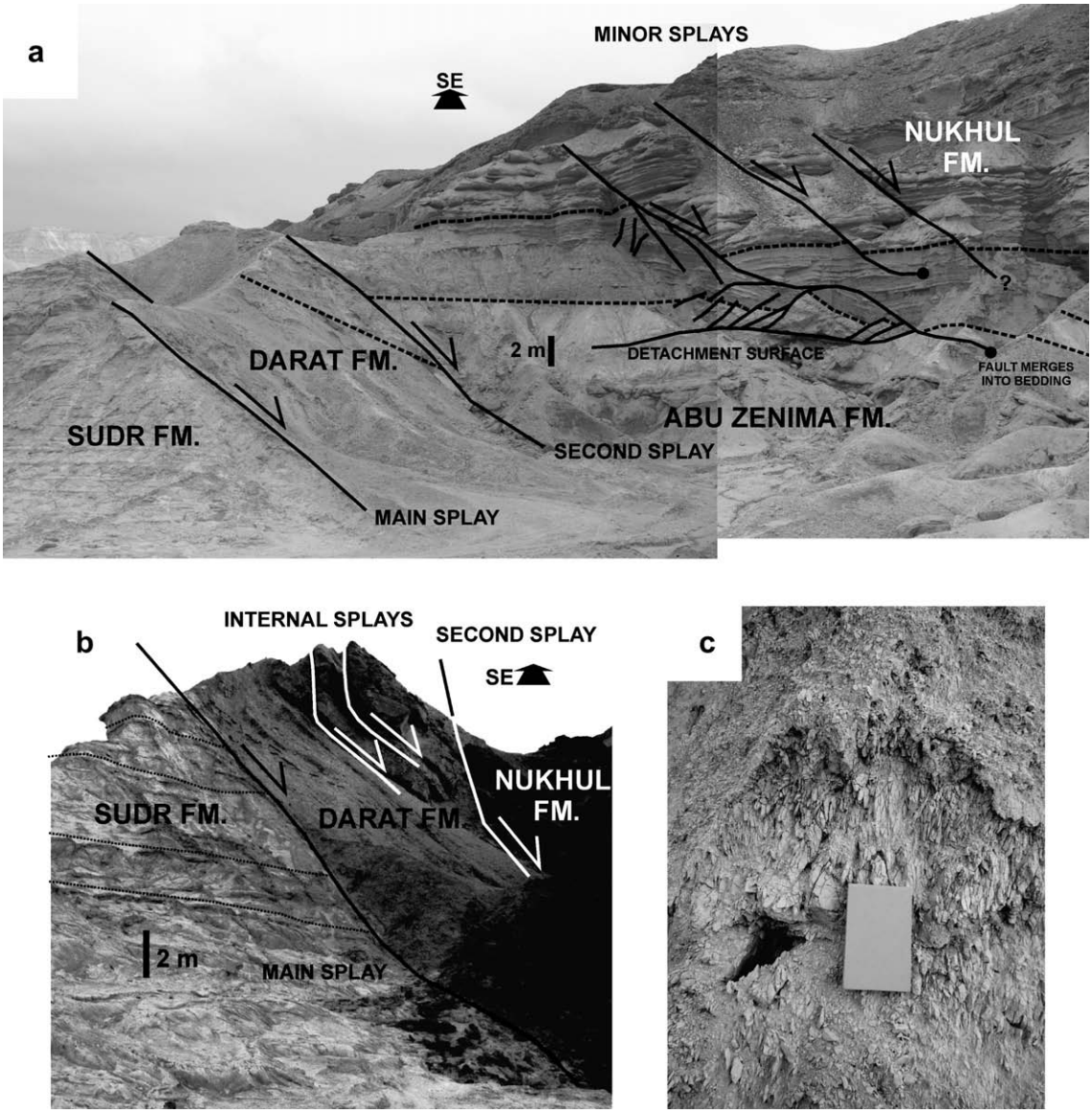

Fig. 9. Geometry and architecture of the Nukhul fault along the east-striking fault that links segments 4 and 5 of the Nukhul fault. (a) Geometry of the Nukhul fault at locality 3 (Fig. 2). A fault-bounded sliver of Darat Formation has pre-rift Sudr Formation in its footwall and syn-rift units in its hanging wall. In the hanging wall of the sliver, syn-rift units are cut by minor normal faults that lose displacement and tip out downward. (b) Geometry of the Nukhul fault at locality 4 (Fig. 2). A sliver of pre-rift Darat Formation is bounded by discrete faults. The fault-bounded sliver contains faults that dip near vertically through limestone units and moderately in mudstone. There is minor folding in the Nukhul Formation in the immediate hanging wall of the rider block. (c) Damage zone of fractured Sudr Formation chalk in the footwall of the Nukhul fault at locality 4.

(50–60°) through the relatively competent Sudr and Matulla formations (Fig. 10a). Faults dip at 20–30° through the relatively weak, clay-rich Duwi Formation, or form bedding-parallel detachments within clay-rich horizons (Fig. 10a). The Duwi Formation is intensely folded and highly variable in thickness across the outcrop, and is interpreted to represent a bedding-parallel detachment. Where faults have small displacements (<1 m or so), they can no longer be traced as discrete planes where they pass into clay-rich units, and are confined to more competent units (Fig. 10a). In this case, deformation in the weak layers is taken up by bedding-parallel detachments. Fault rock at this locality typically comprises clay smear 2–10 cm thick, bounded by paired slip surfaces; no damage zone is developed, as exemplified by the fault shown in Fig. 10b.

5.2.2. The damage zone in syn-rift strata

In the southern part of the study area, an array of approximately east-striking antithetic faults comprise a damage zone in syn-rift strata in the footwall of the Baba-Markha fault, within 1 km of the fault trace (Fig. 2; Fig. 4e). The faults occur in the southward-dipping limb of a fault-parallel monocline in the footwall of the Baba-Markha fault. Analysis of throw distribution patterns has shown that the faults probably initiated during deposition of the Nukhul Formation, possibly at roughly the time the Baba-Markha fault became a surface-breaking structure (Wilson et al., 2009). Fault spacing in the damage zone is on the order of 100–200 m (Fig. 4e). In contrast to the damage zone observed at locality 3, faults are generally straight and steep. Faults A, B, C and D labelled on Fig. 4e are described below.

Fault A (locality 6; Figs. 2 and 11a) is an approximately east-striking fault exposed approximately 1 km to the northwest of the Baba-Markha fault (Fig. 4e). Paired slip surfaces define a fault zone approximately 1.5 m wide (Fig. 12a). Total displacement across the fault zone is approximately 2 m, of which approximately 1.5 m is on the hanging wall slip surface and approximately 0.5 m on the

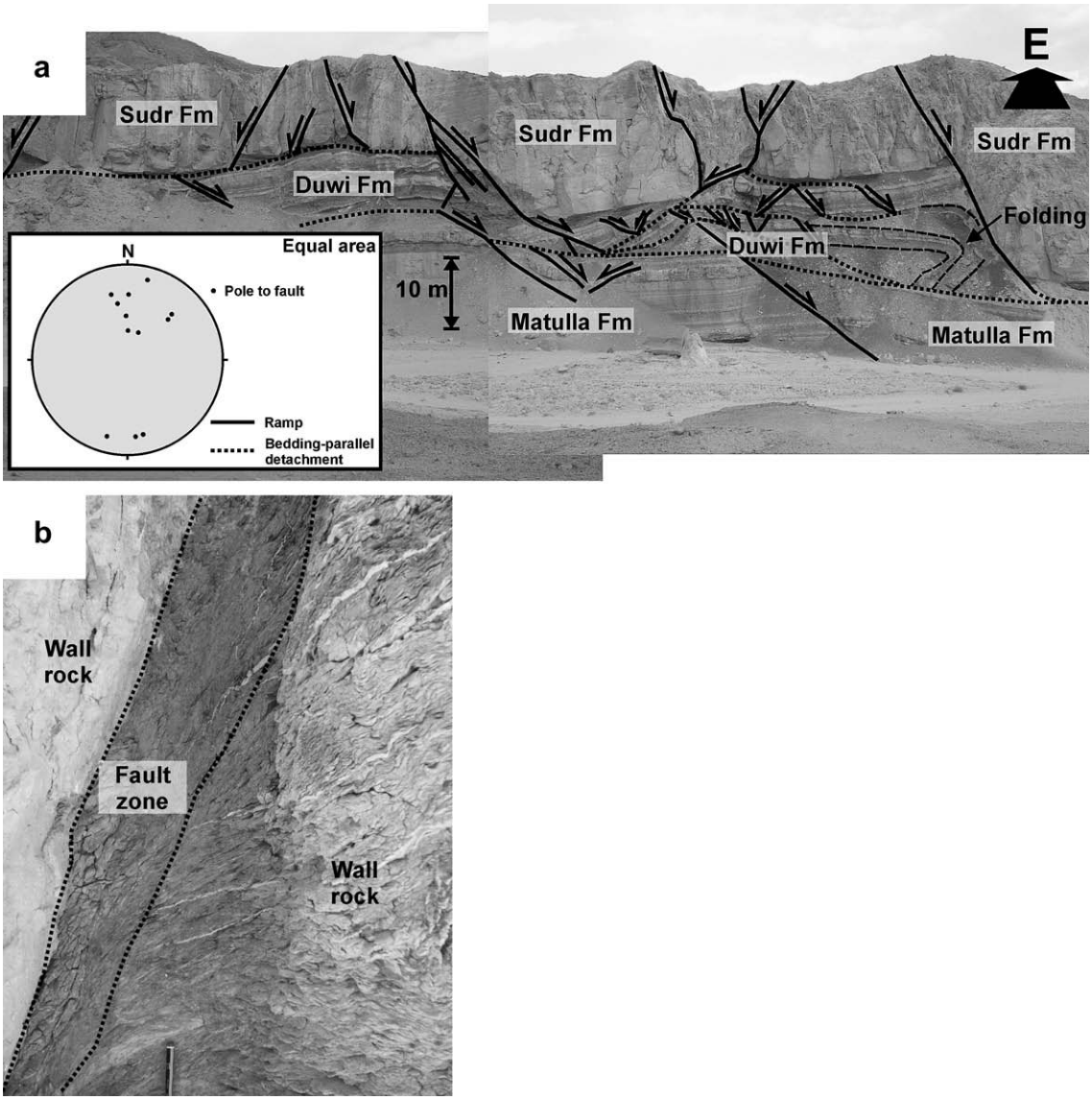

Fig. 10. Geometry and architecture of damage zone faults cutting pre-rift strata in the footwall of the Baba-Markha fault (locality 5, Fig. 2). (a) Geometry of faults. (b) Fault zone showing development of clay smear, typical of the faults at this locality.

footwall slip surface. The fault zone in between the slip surfaces is undeformed and intact, apart from sparse internal minor faults parallel to the fault zone margins (Fig. 12a). The bounding slip surfaces themselves are discrete and do not contain any fault rock.

Fault B (locality 7; Figs. 2 and 11b) is an east-striking low-angle (dip approximately 30°) fault exposed approximately 900 m to the northwest of the Baba-Markha fault. Displacement on the fault is approximately 20 m. The fault cuts all the exposed stratigraphy of the Nukhul Formation, suggesting that it was active until relatively late in the history of the half-graben. The fault zone is well exposed at two points, labelled (c) and (d) on Fig. 11b. The fault zone consists of scaly shale bounded by paired slip surfaces. At point (c), the fault zone is approximately 1–2 cm wide (Fig. 11c), while at point (d) it is approximately 20 cm wide (Fig. 11d).

Fault C (locality 8; Figs. 2 and 11e) is exposed approximately 650 m north of the Baba-Markha fault. It strikes approximately northeast and dips approximately 60° to the northwest. The fault loses displacement upward, and displacement abruptly decreases to zero at the base of a distinctive package of tidal channel sandstone within the upper part of the Nukhul Formation (Figs. 4e and 11e). The fault juxtaposes white lacustrine limestone and fluvial conglomerate (Abu Zenima Formation) in the footwall against fluvial conglomerate, and tidally influenced mudstone and sandstone (Nukhul Formation), in the hanging wall (Fig. 11e). Normal displacement on the fault is estimated at 8–10 m. The main fault consists of a single, sharp, discrete fault plane (Fig. 11f) with no discernible fault rock.

Fault D (locality 9; Figs. 2, 11g) is a roughly east-striking fault exposed approximately 350 m northwest of the Baba-Markha fault (Figs. 2, 11g). The fault is straight and maximum displacement is approximately 25 m. The fault cuts all the preserved Nukhul Formation stratigraphy, and analysis of throw distribution suggests that the fault initiated in Nukhul time, or later (Wilson et al., 2009). The main fault juxtaposes green-grey marl of the basal Nukhul Formation in the footwall against sand-dominated tidal units of the Nukhul Formation in the hanging wall (Fig. 11h). The fault zone, bounded by paired slip surfaces, is between 10 and 15 cm wide. It consists of fault breccia containing fragments of intact Nukhul Formation sandstone up to 3 cm across in a matrix of loose sand grains.

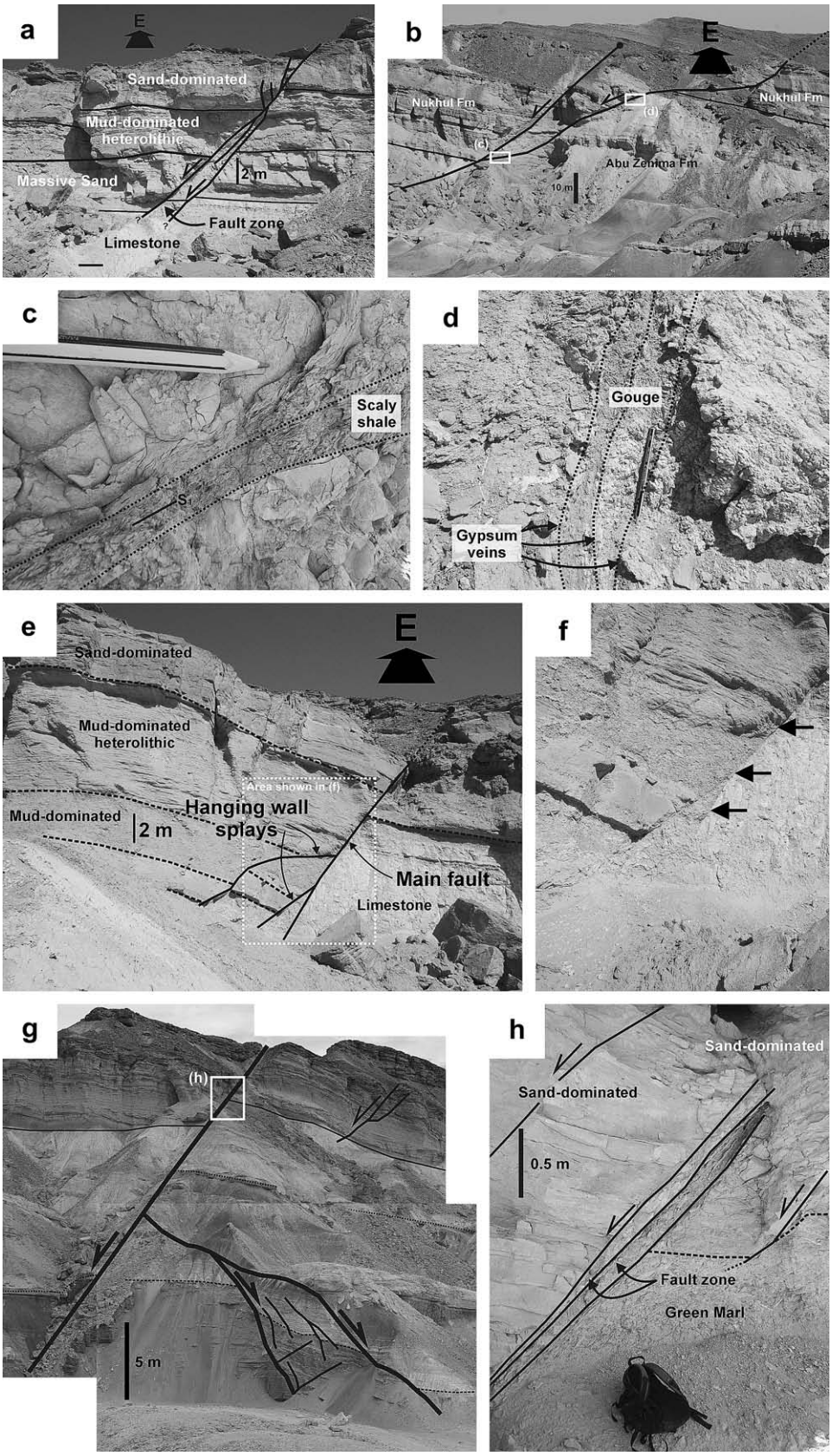

Fig. 11. Antithetic normal faults forming the footwall damage zone of the Baba-Markha fault, as exposed in syn-rift strata: see Fig. 4 for locations of the faults. (a) Overall geometry and architecture of Fault A. (b) Overall geometry of Fault B. (c) Architecture of Fault B at point (c) in Fig. 11b. The fault zone consists of scaly shale with a fault-parallel foliation. No damage zone is developed. (d) Architecture of Fault B at point (d) in Fig. 11b. The fault zone consists of damage zones of scaly shale separated by the fault plane, which contains a thin gypsum vein. The damage zones are also separated from intact protolith by thin gypsum veins. (e) Overall geometry of Fault C, showing splays in the fault hanging wall. (f) Detail of the fault, showing that the fault consists of a discrete fault plane with no core or damage zone development at the scale of observation. (g) Overall geometry of Fault D, including minor antithetic faults in the footwall of Fault D. (h) Detail of Fault D (location shown in Fig. 11 g).

Propa-gation	Juxta-position	Fault zone	Damage zone	Deformation mechanisms
Surface breaking fault	Syn-rift against syn-rift	Simple fault plane, or narrow zone (<10 cm) of cataclastic fault rock	None, or zone of minor faults up to several tens of metres wide Largely confined to hangingwall	Cataclasis Fault slip Drag folding
	Pre-rift agaijnst syn-rift	Narrow zone (<10 cm) of cataclastic fault rock	Zone of minor faults up to several tens of metres wide Largely confined to hangingwall	Cataclasis Fault slip Drag folding
Blind fault	Pre-rift against pre-rift	Up to 10 m wide, containing blocks of competent wall rock up to 1.5 m across in a matrix of deformed shale cut by clay gouge zones	Hangingwall: approx. 100m of layer-parallel slip in shale horizons and minor normal faults that have been passively rotated during monocline formation Footwall: no damage zone, or a few metres of minor faulting near segment linkage points	Fault propagation folding Layer-parallel slip Cataclastic flow Fault slip

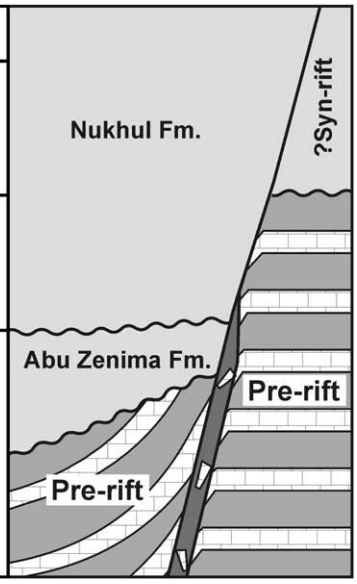

Fig. 12. Summary of fault and damage zone characteristics, and deformation mechanisms, observed at different structural levels in faults of the Nukhul half-graben.

6. Discussion

6.1. Evolution of the geometry and architecture of the Nukhul fault

Our observations of fault geometry, architecture and deformation mechanisms are summarised in Fig. 12, while the evolution of the Nukhul fault system is summarised below (Fig. 13). Interpretations of isopach maps suggest that the Nukhul fault was buried during deposition of the Abu Zenima Formation, and broke the surface during deposition of the Nukhul Formation (Fig. 5c and d); hence the Nukhul fault propagated upward during its development. Our observations show that the Nukhul fault has a hanging wall monocline at the level of the pre-rift and Abu Zenima Formation, but not at the level of the Nukhul Formation. This suggests that faulting was accompanied by fault-propagation folding, until the monocline was breached by the growing fault. These observations are consistent with previous work showing that the development of fault-propagation folds can be modelled using a trishear kinematic model, in which deformation occurs in a triangular zone of distributed shear attached to the fault tip (Allmendinger, 1998; Finch et al., 2003; Fig. 13a). Once the fault tip reaches the surface, fault-propagation folding ceases, and subsequent deformation is dominated by surface faulting (Willsey et al., 2002).

The Nukhul fault initiated, together with steeply dipping minor faults in the hanging wall, and propagated upward. An upward-widening monoclinal fault-propagation fold formed above the fault tip (Withjack et al., 1990; Allmendinger, 1998; Fig. 13a, b), as observed in Fig. 6. As the fault continued to accrue displacement, the monocline amplified (Fig. 13c). Reverse-sense layer-parallel shear zones within the shale units of the Darat Formation in the hanging wall (Fig. 4a) formed as a result of folding in the monocline being accommodated by flexural slip. Steep antithetic faults continued to form ahead of the propagating fault tip. These steepened upwards and ultimately became high-angle reverse faults (Fig. 6b; Withjack et al., 1990; Allmendinger, 1998). During rotation of bedding as the monocline amplified, pre-existing antithetic faults were passively rotated into low-angle orientations, and synthetic faults were rotated through vertical to become high-angle reverse faults (Figs. 7 and 8; Sharp et al., 2000b). Displacement continued to accrue on the fault, and the syn-rift Abu Zenima Formation began to accumulate in the monoclinal flexure (Fig. 13d). Following deposition of the Abu Zenima Formation, the Nukhul fault breached the surface. At that point, fault-propagation folding ceased (although folding due to frictional normal drag may have continued; see Fig. 9b). A period of surface faulting then began (Fig. 13e; Willsey et al., 2002), and further deformation was accommodated largely by surface faulting until the fault ceased to be active.

The evolution of the Nukhul fault from a buried structure with associated formation of a fault-propagation monocline, to a surface-breaking structure associated with surface faulting, contributes to the contrasting architectural style of the fault zone at different structural levels. In the volume of rock that was part of a trishear zone before the fault breached the surface, layer-parallel shear, resulting from flexural slip on relatively weak horizons, is enhanced during monocline formation (Cooke and Pollard, 1997). This layer-parallel shear along bedding planes can create asperities adjacent to the fault zone. These asperities can be broken off by subsequent deformation and become incorporated into the fault zone as isolated blocks of wall rock (Watterson et al., 1998). This effect can be enhanced because faults in multilayered rocks are typically vertically segmented (Rykkelid and Fossen, 2002). Rotation of beds occurs where the fault segments overlap, leading to layer-parallel shear and the development of asperities (Watterson et al., 1998). As bedding approaches parallelism with the fault zone, shale layers will be preferentially smeared into the fault zone. These combined processes will result in a relatively wide, shaly fault zone containing dismembered blocks of competent strata, as observed at locality 1 (Figs. 6b, 12). During deposition of the Nukhul Formation, the Nukhul fault had breached the surface and fault-propagation folding was no longer active; deformation was instead dominated by surface faulting (Willsey et al., 2002; Fig. 13). Hence the processes described above are not important at this structural level, resulting in a fault zone that is relatively narrow and does not contain large thicknesses of deformed shale.

Previous work has shown that the Nukhul fault developed from a series of initially isolated precursor fault strands, which grew laterally and probably became linked prior to deposition of the Nukhul Formation, within 2.5 m.y. of the onset of rifting (Gawthorpe et al., 2003; Wilson et al., 2009). The short, east-striking fault that links segments 1 and 2 of the Nukhul fault is associated with folds perpendicular to the strike of the Nukhul fault

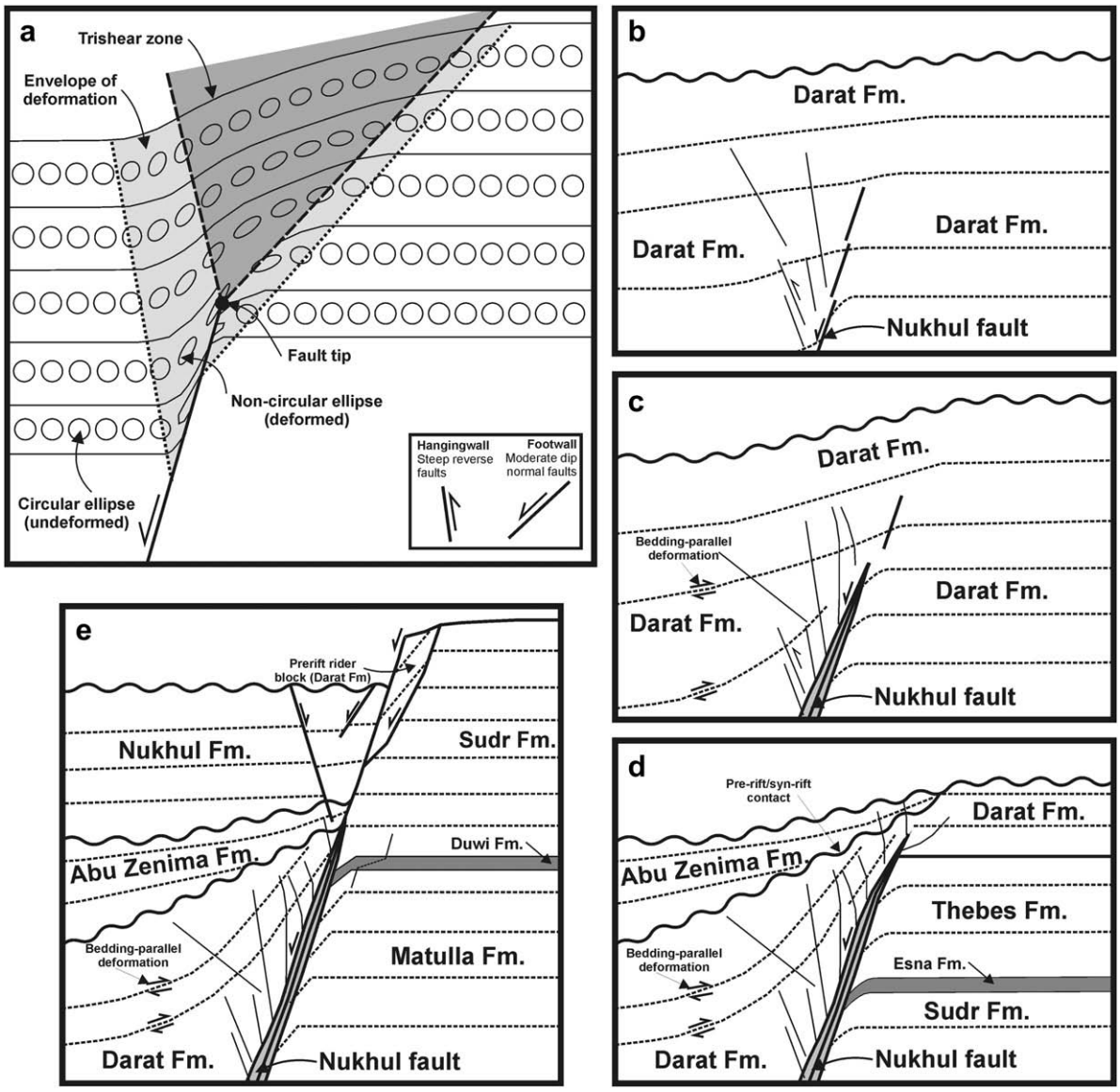

Fig. 13. Summary of propagation and architectural evolution of the Nukhul fault. (a) Trishear model of deformation around a propagating normal fault tip. Distributed deformation occurs in a triangular zone with a vertex at the fault tip. As the fault propagates upward, the trishear zone also moves upward, leaving behind an approximately triangular envelope of deformed rock. When the fault tip reaches the surface, trishear deformation ceases, as there is no longer any trishear zone above the fault tip. Modified after Allmendinger (1998). (b) Initiation of the Nukhul fault. (c) Continued propagation of the Nukhul fault upward through the pre-rift units. (d) As fault propagation continues, syn-rift sediments of the Abu Zenima Formation begin to be deposited in the surface flexure caused by folding ahead of the propagating fault tip. (e) After the fault tip breaches the surface, fault-propagation folding ceases and a period of surface faulting begins.

(Fig. 5a, b), representing variations in displacement (Wilson et al., 2009). It is suggested that this linking segment represents a breached relay (Peacock and Sanderson, 1991, 1994; Schlische, 1995; Janecke et al., 1998; Walsh et al., 1999; Bonson et al., 2007). This locality is associated with a 50 m wide brittle damage zone of synthetic normal faults. The normal faults in the damage zone are seen to tip out downward at approximately the level of the top of the Abu Zenima Formation (Fig. 9a). This suggests that the hanging wall damage zone faults initiated within the Nukhul formation, and propagated both upward and downward (and laterally) through the syn-rift. If segments 4 and 5 of the Nukhul fault linked approximately at the beginning of Nukhul deposition (Wilson et al., 2009), these damage zone faults could be related to the relay breaching process. The presence of a relatively thick damage zone containing normal faults along the linking segment is consistent with observations from elsewhere that breached relays tend to have high fault densities (e.g. Walsh et al., 1999; Bonson et al., 2007).

At locality 1, there is a sharp bend in the trace of the Nukhul fault (Fig. 2). Although the bend might represent the position of a breached relay, there is no evidence to support that interpretation from fault-perpendicular folds representing along-strike variations in displacement (Fig. 5b). We suggest that either the linkage of segments 1 and 2 took place very early in the history of the half-graben (Wilson et al., 2009), or that the bend was inherited from a pre-existing structure that was reactivated during rifting (Montenat et al., 1988; Younes and McClay, 2002; Bull et al., 2006). The anomalous width of the fault zone at this locality, and the presence of footwall splays, are probably related to strain accommodation at the fault bend (e.g. Bonson et al., 2007).

6.2. Lithological control on fault development

Our observations suggest a significant component of lithological control on fault geometry and architecture in the Wadi Nukhul

area, both in terms of rock type, and the state of lithification of the rock at the time of deformation.

Along the Nukhul fault, changes in geometry and architectural style are associated with changes in the footwall and hanging wall lithologies. Along segments 1 and 2 of the Nukhul fault, where the fault juxtaposes the pre-rift Matulla (calcareous sandstone interbedded with mudstone) and Darat (limestone interbedded with mudstone) formations, the fault zone is characterised by an approximately 10 m wide zone of dismembered competent (calcareous sandstone and limestone) beds in a matrix of deformed shale (Fig. 6b). The presence of identifiable Matulla Formation blocks on the footwall side of the fault, and Darat Formation blocks on the hanging wall side of fault, shows that fault zone material was mainly derived from the adjacent wall rocks. The width (5–10 m) and architectural style of the fault zone is broadly consistent along these segments, a strike length of approximately 1.2 km. Along segments 1, 2 and 3 of the Nukhul fault, where the fault juxtaposes the pre-rift Sudr Formation against the syn-rift Abu Zenima and Nukhul formations, the fault zone is generally not well exposed, but is characterised by a single discrete fault zone less than 2 m wide, with minor faults up to approximately 200 m into the hanging wall (Fig. 2). This geometry and architecture is broadly consistent along a strike length of 3.5 km, apart from along the short east-striking segment that links segments 1 and 2 of the Nukhul fault, which represents a breached relay (see Section 6.1).

Faults in the damage zone of the Baba-Markha fault show different characteristics between exposures in pre-rift and syn-rift units. Complex fault geometries occur in pre-rift units, where faults dip steeply through competent sandstone and limestone units, and flatten and merge into detachment surfaces in relatively incompetent shale layers (Fig. 10). In contrast, the faults in the syn-rift are generally very straight and sharp, with zones of gouge or fault breccia up to a few tens of cm thick, or no fault rock present (Fig. 11). Despite cutting lithologies that would be expected to show different levels of competence (i.e. mudstone, sandstone and limestone units), fault geometries are generally relatively simple in syn-rift units.

These observations can be explained by the influence of the state of lithification of the sedimentary succession at the time of faulting on the competence contrast between the different lithologies. Previous studies have shown that in unlithified rocks, the most important process of clay smear formation is 'shear smearing' (Lindsay et al., 1993; Yielding et al., 1997) or 'preferred smearing' (van der Zee and Urai, 2005), which is dependent on the contrast in competence between sandstone and shale (Sperrevik et al., 2000); sandstone beds tend to fracture in a brittle manner, while shale tends to shear ductilely under the same conditions. However, at shallow levels under low confining pressures, shear smearing is inhibited because of relatively strong electrostatic forces between clay grains (e.g. Jones, 1994).

Low confining pressures and lack of lithification at shallow depths lead to fault zones that lack fault rock (e.g. those shown in Fig. 11a, e and f). In these examples, the faults abruptly tip out at erosional surfaces within the Nukhul Formation (Fig. 4e), suggesting that they ceased to be active during Nukhul time. Other faults in the Baba-Markha fault damage zone do contain cataclastic fault rocks (Fig. 11c, d and h). However, in these examples, the faults do not tip out within the Nukhul Formation section (Fig. 4e), suggesting that they continued to be active throughout Nukhul time. Formation of cataclastic fault rock in these faults can be attributed to the faults remaining active during lithification of the syn-rift units.

The hanging wall of the Nukhul fault contains a relatively high density of minor antithetic and synthetic faults, while minor faults are rare to absent in the footwall (Fig. 2). This might be a result of deformation in lithified units in the footwall 'switching off' as they are juxtaposed against poorly lithified syn-rift sediments in the hanging wall (e.g. Bonson et al., 2007). However, there is little deformation in the footwall of the Nukhul fault at any observed structural level, and the hanging wall of the fault is highly deformed even where lithified rocks are juxtaposed against lithified rocks (i.e. along segments 1 and 2 of the Nukhul fault). We suggest that the lack of deformation in the footwall may relate to the configuration of the trishear zone, with distributed deformation mainly confined to the hanging wall, as in the analogue model experiments of Withjack et al. (1990) and trishear numerical modelling of Allmendinger (1998).

6.3. Implications for fluid flow

The observations reported in this paper have some implications for fluid flow. In faults that are initially blind and propagate upward to breach the surface, there are likely to be significant vertical changes in fault architecture, as a result of differing deformation mechanisms (Fig. 12). In the Nukhul fault, a 5–10 m wide zone containing shale smear and gouge is developed along the portion of the fault that was active while the fault tip remained buried. A much thinner (<20 cm), and less continuous, zone of cataclastic fault rock is present at higher levels of the fault that were active after the fault breached the surface. Hence there is likely to be a significant deterioration in fault seal integrity between the buried and surface breaching portions of the fault. It is also clear that timing of lithification with respect to fault activity is critically important. In this study, faults that died out during Nukhul Formation deposition (e.g. faults A and C within the Baba-Markha fault damage zone: Fig. 11a, e and f) contain no observable fault rock. Faults that continued to be active throughout Nukhul Formation deposition contain thin zones of cataclastic fault rock (e.g. faults B and D in the Baba-Markha fault damage zone: Fig. 11b–d, g and h). Hence faults A and C are likely to have less sealing capacity than faults B and D. During the evolution of fault population, faults initiate, grow, interact, link and die out (Cartwright et al., 1995; Cowie et al., 2000; Gawthorpe et al., 2003). The timing of all these processes, both in relation to timing of surface breaching and timing of lithification, is likely to have a profound influence on the permeability architecture of the resulting fault array.

7. Conclusions

The geometry and architecture of the Nukhul fault zone is controlled by lithology, inherited pre-existing structures, and the history of fault segmentation, growth and linkage. Where the fault juxtaposes the pre-rift Matulla and Darat formations, it consists of a single zone of intense deformation with a significant monocline in the hanging wall and much more limited folding in the footwall. Where the Nukhul fault juxtaposes the pre-rift Sudr Formation against syn-rift units, the fault zone is characterised by a single discrete fault zone less than 2 m wide, with minor faults within approximately 200 m into the hanging wall, and no significant monocline developed. The evolution of the fault from a buried structure with associated fault-propagation folding, to a surface-breaking structure with associated surface faulting, has led to enhanced bedding-parallel slip at lower levels in the succession that is absent at higher levels due to the vertical variation in lithification. Strain is enhanced at breached relay ramps along the fault (e.g. between segments 4 and 5; Fig. 9), and at bends along the fault that were inherited from pre-existing structures that were reactivated during rifting (e.g. between segments 1 and 2; Fig. 6). Faults within the footwall damage zone of the Baba-Markha fault in the pre-rift show clay smear and ramp-flat geometries (Fig. 10).

Bedding-parallel distributed shear zones in shale horizons link to steep, discrete faults in relatively competent horizons. In contrast, faults in the damage zone in the syn-rift are generally straight and discrete (Fig. 11), although they pass through sand-dominated and mudstone-dominated horizons that would be expected to show contrasting competency. These architectural variations are the result of different responses to deformation occurring at shallow levels in the unlithified sediment, where competence contrast is likely to be low, and at deeper levels in lithified rock, where competence contrasts are likely to be high. Faults that die out during Nukhul Formation deposition contain no observable fault rock, while faults that continued to be active throughout Nukhul deposition contain thin zones of cataclastic fault rock. This difference is a result of timing of deformation relative to timing of lithification. The timing of fault growth, segmentation and linkage, relative to surface breaching and timing of lithification, is likely to have a profound influence on the permeability architecture of the resulting fault array.

Acknowledgments

Funding for this work was provided by Norsk Hydro and Statoil (now StatoilHydro) and ConocoPhillips through The Rift Analogues Project (TRAP) consortium at the University of Manchester. Schlumberger provided licenses for Petrel. Constructive reviews by J.J. Walsh, G. Yielding and C. Bonson considerably improved the quality of the manuscript. Interpretation of LIDAR data and field mapping was based on earlier NERC-funded work by two of the authors (IRS and RLG). Sayed, Gamal and Bilal Gooda assisted with field logistics.

References

Allmendinger, R.W., 1998. Inverse and forward numerical modeling of trishear fault-propagation folds. Tectonics 17, 640–656.
Bellian, J.A., Kerans, C., Jennette, D.C., 2005. Digital outcrop models: applications of terrestrial scanning LIDAR technology in stratigraphic modeling. Journal of Sedimentary Research 75, 166–176.
Bonson, C.G., Childs, C., Walsh, J.J., Schöpfer, M.P.J., Carboni, V., 2007. Geometric and kinematic controls on the internal structure of a large normal fault in massive limestones: the Maghlaq Fault, Malta. Journal of Structural Geology 29, 336–354.
Bosworth, W., Huchon, P., McClay, K., 2005. The Red Sea and Gulf of Aden basins. Journal of African Earth Sciences 43, 334–378.
Bull, J.M., Barnes, P.M., Lamarche, G., Sanderson, D.J., Cowie, P.A., Taylor, S.K., Dix, J.K., 2006. High-resolution record of displacement accumulation on an active normal fault: implications for models of slip accumulation during repeated earthquakes. Journal of Structural Geology 28, 1146–1166.
Cardozo, N., Allmendinger, R.W., Morgan, J.K., 2005. Influence of mechanical stratigraphy and initial stress state on the formation of two fault-propagation folds. Journal of Structural Geology 27, 1954–1972.
Cartwright, J.A., Trudgill, B.D., Mansfield, C.S., 1995. Fault growth by segment linkage: an explanation for scatter in maximum displacement and trace length data from the Canyonlands Grabens of SE Utah. Journal of Structural Geology 17, 1319–1326.
Childs, C., Nicol, A., Walsh, J.J., Watterson, J., 1996a. Growth of vertically segmented normal faults. Journal of Structural Geology 18, 1389–1397.
Childs, C., Watterson, J., Walsh, J.J., 1996b. A model for the structure and development of fault zones. Journal of the Geological Society 153, 337–340.
Cooke, M.L., Pollard, D.D., 1997. Bedding-plane slip in initial stages of fault-related folding. Journal of Structural Geology 19, 567–581.
Cowie, P.A., Gupta, S., Dawers, N.H., 2000. Implications of fault array evolution for synrift depocentre development: insights from a numerical fault growth model. Basin Research 12, 241–261.
Dominic, J.B., McConnell, D.A., 1994. The influence of structural lithic units in fault-related folds, Seminoe Mountains, Wyoming, U.S.A. Journal of Structural Geology 16, 769–779.
Erickson, S.G., 1996. Influence of mechanical stratigraphy on folding vs. faulting. Journal of Structural Geology 18, 443–450.
Finch, E., Hardy, S., Gawthorpe, R., 2003. Discrete element modelling of contractional fault-propagation folding above rigid basement fault blocks. Journal of Structural Geology 25, 515–528.
Garfunkel, Z., Bartov, Y., 1977. The tectonics of the Suez Rift. Geological Survey of Israel Bulletin 71, 1–41.
Gawthorpe, R.L., Leeder, M.R., 2000. Tectono-sedimentary evolution of active extensional basins. Basin Research 12, 195–218.
Gawthorpe, R.L., Jackson, C.A.L., Young, M.J., Sharp, I.R., Moustafa, A.R., Leppard, C.W., 2003. Normal fault growth, displacement localisation and the evolution of normal fault populations: the Hammam Faraun fault block, Suez rift, Egypt. Journal of Structural Geology 25, 883–895.
Hancock, P.L., 1985. Brittle microtectonics: principles and practice. Journal of Structural Geology 7, 437–457.
Heynekamp, M.R., Goodwin, L.B., Mozley, P.S., 1999. Controls on fault-zone architecture in poorly lithified sediments, Rio Grande rift, New Mexico: implications for fault-zone permeability and fluid flow. In: Haneberg, W.C., Mozley, P.S., Moore, J.C., Goodwin, L.B. (Eds.), Faults and Subsurface Fluid Flow in the Shallow Crust. Geophysical Monograph 113, pp. 27–49.
Jackson, C.A.L., Gawthorpe, R.L., Sharp, I.R., 2006. Style and sequence of deformation during extensional fault-propagation folding: examples from the Hammam Faraun and El-Qaa fault blocks, Suez Rift, Egypt. Journal of Structural Geology 28, 519–535.
Janecke, S.U., Vandenburg, C.J., Blankenau, J.J., 1998. Geometry, mechanisms and significance of extensional folds from examples in the Rocky Mountain Basin and Range province, U.S.A. Journal of Structural Geology 20, 841–856.
Jones, M., 1994. Mechanical principles of sediment deformation. In: Maltman, A. (Ed.), The Geological Deformation of Sediments. Chapman and Hall, London, pp. 37–71.
Khalil, S.M., McClay, K.R., 2002. Extensional fault-related folding, northwestern Red Sea, Egypt. Journal of Structural Geology 24, 743–762.
Kim, Y.–S., Peacock, D.C.P., Sanderson, D.J., 2004. Fault damage zones. Journal of Structural Geology 26, 503–517.
Krebs, W.N., Wescott, W.A., Nummedal, D., Gaafar, I., Azazi, G., Karamat, S., 1997. Graphic correlation and sequence stratigraphy of Neogene rocks in the Gulf of Suez. Bulletin de la Société Géologique de France 168, 63–71.
Lindsay, N.G., Murphy, F.C., Walsh, J.J., Watterson, J., 1993. Outcrop studies of shale smears on fault surfaces. In: Flint, S.S., Bryant, I.D. (Eds.), The Geological Modelling of Hydrocarbon Reservoirs and Outcrop Analogues. Special Publications of the International Association of Sedimentologists 15, pp. 113–123.
Lyberis, N., 1988. Tectonic evolution of the Gulf of Suez and Gulf of Aqaba. Tectonophysics 153, 209–220.
McGrath, A.G., Davison, I., 1995. Damage zone geometry around fault tips. Journal of Structural Geology 17, 1011–1024.
Montenat, C., D'Estevou, P.O., Purser, B., Burollet, P.F., Jarrige, J.J., Orszag-Sperber, F., Philobbos, E., Plaziat, J.C., Prat, P., Richert, J.P., Roussel, N., Thiriet, J.P., 1988. Tectonic and sedimentary evolution of the Gulf of Suez and the northwestern Red Sea. Tectonophysics 153, 161–177.
Moustafa, A.R., 1987. Drape folding in the Baba-Sidri area, eastern side of Suez Rift, Egypt. Journal of Geology 31, 15–27.
Moustafa, A.R., 1993. Structural characteristics and tectonic evolution of the east margin blocks of the Suez rift. Tectonophysics 223, 381–399.
Moustafa, A.R., 1996. Internal structure and deformation of an accommodation zone in the northern part of the Suez rift. Journal of Structural Geology 18, 93–107.
Moustafa, A.R., 1997. Controls on the development and evolution of transfer zones: the influence of basement structure and sedimentary thickness in the Suez rift and Red Sea. Journal of Structural Geology 19, 755–768.
Moustafa, A.R., Abdeen, A.R., 1992. Structural setting of the Hammam Faraun fault block, eastern side of the Suez Rift. Journal of the University of Kuweit (Science) 19, 291–310.
Pascoe, R., Hooper, R., Storhaug, K., Harper, H., 1999. Evolution of extensional styles at the southern termination of the Nordland Ridge, mid-Norway; a response to variations in coupling above Triassic salt. In: Fleet, A.J., Boldy, S.A.R. (Eds.), Petroleum Geology of Northwest Europe; Proceedings of the 5th Conference, pp. 83–90.
Patton, T.L., Moustafa, A.R., Nelson, R.A., Abdine, A.S., 1994. Tectonic evolution and structural setting of the Gulf of Suez rift. In: Landon, S.M. (Ed.), Interior Rift Basins. American Association of Petroleum Geologists Memoir 59, pp. 9–55.
Peacock, D.C.P., Sanderson, D.J., 1991. Displacements, segment linkage and relay ramps in normal fault zones. Journal of Structural Geology 13, 721–733.
Peacock, D.C.P., Sanderson, D.J., 1994. Geometry and development of relay ramps in normal fault systems. American Association of Petroleum Geologists Bulletin 78, 147–165.
Pringle, J.K., Howell, J.A., Hodgetts, D., Westerman, A.R., Hodgson, D.M., 2006. Virtual outcrop models of petroleum reservoir analogues: a review of the current state-of-the-art. First Break 24, 33–42.
Rawling, G.C., Goodwin, L.B., Wilson, J.L., 2001. Internal architecture, permeability structure, and hydrologic significance of contrasting fault zone types. Geology 29, 43–46.
Redfern, J., Hodgetts, D., Fabuel-Perez, I., 2007. Digital analysis brings renaissance for petroleum geology outcrop studies in North Africa. First Break 25, 81–87.
Richardson, M., Arthur, M.A., 1988. The Gulf of Suez — northern Red Sea Neogene rift: a quantitative basin analysis. Marine and Petroleum Geology 5, 247–270.
Robson, D.A., 1971. The structure of the Gulf of Suez (Clysmic) rift, with special reference to the eastern side. Journal of the Geological Society of London 127, 247–276.
Rykkelid, E., Fossen, H., 2002. Layer rotation around vertical fault overlap zones: observations from seismic data, field examples, and physical experiments. Marine and Petroleum Geology 19, 181–192.

Schlische, R.W., 1995. Geometry and origin of fault-related folds in extensional basins. American Association of Petroleum Geologists Bulletin 79, 1246–1263.
Schöpfer, M.P.J., Childs, C., Walsh, J.J., 2006. Localisation of normal faults in multilayer sequences. Journal of Structural Geology 28, 816–833.
Schöpfer, M.P.J., Childs, C., Walsh, J.J., Manzocchi, T., Koyi, H.A., 2007. Geometrical analysis of the refraction and segmentation of normal faults in periodically layered sequences. Journal of Structural Geology 29, 318–335.
Sharp, I.R., Gawthorpe, R.L., Underhill, J.R., Gupta, S., 2000a. Fault-propagation folding in extensional settings: examples of structural style and synrift sedimentary response from the Suez rift, Sinai, Egypt. Geological Society of America Bulletin 112, 1877–1899.
Sharp, I.R., Gawthorpe, R.L., Armstrong, B., Underhill, J.R., 2000b. Propagation history and passive rotation of mesoscale normal faults: implications for synrift stratigraphic development. Basin Research 12, 285–306.
Sibson, R.H., 1986. Brecciation processes in fault zones: inferences from earthquake rupturing. Pure and Applied Geophysics 124, 159–175.
Sigda, J.M., Goodwin, L.B., Mozley, P.S., Wilson, J.L., 1999. Permeability alteration in small-displacement faults in poorly lithified sediments: Rio Grande rift, central New Mexico. In: Haneberg, W.C., Mozley, P.S., Moore, J.C., Goodwin, L.B. (Eds.), Faults and Subsurface Fluid Flow in the Shallow Crust. Geophysical Monograph 113, pp. 27–49.
Sperrevik, S., Faerseth, R.B., Gabrielsen, R.H., 2000. Experiments on clay smear formation along faults. Petroleum Geoscience 6, 113–123.
Walsh, J.J., Watterson, J., Bailey, W.R., Childs, C., 1999. Fault relays, bends and branch-lines. Journal of Structural Geology 21, 1019–1026.
Watterson, J., Childs, C., Walsh, J.J., 1998. Widening of fault zones by erosion of asperities formed by bed-parallel slip. Geology 26, 71–74.
Wibberley, C.A.J., Petit, J.P., Rives, T., 2007. The effect of tilting on fault propagation and network development in sandstone–shale sequences: a case study from the Lodève Basin, southern France. Journal of the Geological Society 164, 599–608.
Willsey, S.P., Umhoefer, P.J., Hilley, G.E., 2002. Early evolution of an extensional monocline by a propagating normal fault: 3D analysis from combined field study and numerical modeling. Journal of Structural Geology 24, 651–669.
Wilson, P., 2008. Comment on 'Architecture, gods and gobbledygook'. Journal of Structural Geology 30, 1614.
Wilson, P., Hodgetts, D., Rarity, F., Gawthorpe, R.L., Sharp, I.R., 2009. Structural geology and 4D evolution of a half-graben: new digital outcrop modelling techniques applied to the Nukhul half-graben, Suez rift, Egypt. Journal of Structural Geology 31, 328–345.
Withjack, M.O., Olson, J., Peterson, E., 1990. Experimental models of extensional forced folds. American Association of Petroleum Geologists Bulletin 74, 1038–1054.
Yielding, G., Freeman, B., Needham, D.T., 1997. Quantitative fault seal prediction. American Association of Petroleum Geologists Bulletin 81, 897–917.
Younes, A.I., McClay, K.R., 2002. Development of accommodation zones in the Gulf of Suez-Red Sea Rift, Egypt. Bulletin of the American Association of Petroleum Geologists 86, 1003–1026.
van der Zee, W., Urai, J.L., 2005. Processes of normal fault evolution in a siliciclastic sequence: a case study from Miri, Sarawak, Malaysia. Journal of Structural Geology 27, 2281–2300.